



UvA-DARE (Digital Academic Repository)

Effect of particle collisions in dense suspension flows

Düring, G.; Lerner, E.; Wyart, M.

DOI

[10.1103/PhysRevE.94.022601](https://doi.org/10.1103/PhysRevE.94.022601)

Publication date

2016

Document Version

Final published version

Published in

Physical Review E

[Link to publication](#)

Citation for published version (APA):

Düring, G., Lerner, E., & Wyart, M. (2016). Effect of particle collisions in dense suspension flows. *Physical Review E*, *94*(2), [022601]. <https://doi.org/10.1103/PhysRevE.94.022601>

General rights

It is not permitted to download or to forward/distribute the text or part of it without the consent of the author(s) and/or copyright holder(s), other than for strictly personal, individual use, unless the work is under an open content license (like Creative Commons).

Disclaimer/Complaints regulations

If you believe that digital publication of certain material infringes any of your rights or (privacy) interests, please let the Library know, stating your reasons. In case of a legitimate complaint, the Library will make the material inaccessible and/or remove it from the website. Please Ask the Library: <https://uba.uva.nl/en/contact>, or a letter to: Library of the University of Amsterdam, Secretariat, Singel 425, 1012 WP Amsterdam, The Netherlands. You will be contacted as soon as possible.

Effect of particle collisions in dense suspension flows

Gustavo Düring,¹ Edan Lerner,² and Matthieu Wyart³

¹*Facultad de Física, Pontificia Universidad Católica de Chile, Casilla 306, Santiago, Chile*

²*Institute for Theoretical Physics, Institute of Physics, University of Amsterdam, Science Park 904, 1098 XH Amsterdam, the Netherlands*

³*Institute of Theoretical Physics, École Polytechnique Fédérale de Lausanne, CH-1015 Lausanne, Switzerland*

(Received 23 February 2016; published 4 August 2016)

We study nonlocal effects associated with particle collisions in dense suspension flows, in the context of the Affine Solvent Model, known to capture various aspects of the jamming transition. We show that an individual collision changes significantly the velocity field on a characteristic volume $\Omega_c \sim 1/\delta z$ that diverges as jamming is approached, where δz is the deficit in coordination number required to jam the system. Such an event also affects the contact forces between particles on that same volume Ω_c , but this change is modest in relative terms, of order $f_{\text{coll}} \sim \bar{f}^{0.8}$, where \bar{f} is the typical contact force scale. We then show that the requirement that coordination is stationary (such that a collision has a finite probability to open one contact elsewhere in the system) yields the scaling of the viscosity (or equivalently the viscous number) with coordination deficit δz . The same scaling result was derived [E. DeGiuli, G. Düring, E. Lerner, and M. Wyart, *Phys. Rev. E* **91**, 062206 (2015)] via different arguments making an additional assumption. The present approach gives a mechanistic justification as to why the correct finite size scaling volume behaves as $1/\delta z$ and can be used to recover a marginality condition known to characterize the distributions of contact forces and gaps in jammed packings.

DOI: [10.1103/PhysRevE.94.022601](https://doi.org/10.1103/PhysRevE.94.022601)

I. INTRODUCTION

Suspensions are complex fluids consisting of solid particles immersed in a viscous liquid. The presence of solid particles affects flows, especially when the concentration of particles or the so-called packing fraction ϕ becomes large. In the dilute limit Einstein proved that the presence of particles leads to a linear increase of the viscosity η with ϕ [1]. However, the dilute regime breaks down upon densification as steric-hindrance effects become dominant. At larger packing fractions [2,3] the viscosity even diverges at the jamming point ϕ_c where the suspension jams into an amorphous solid. Critical exponents governing the rheology of dense suspensions as well as a diverging correlation length scale have been observed in experiments [2–6] and in numerical models [7–16].

In the context of frictionless particles, we have proposed together with others a microscopic description that predicts both the explosion of the correlation length of velocity fluctuations [17] as well as the critical rheological properties of both overdamped and inertial flows [18]. This approach has received recent numerical [18,19] and empirical [20] support. However, it makes an assumption on the nature of flowing configurations, thought to be similar to slightly perturbed jammed configurations. It also predicts that the finite size volume scales as $1/\delta z$, which differs (except in two dimensions) from the naive estimate ξ^d , where $\xi \sim 1/\sqrt{\delta z}$ is the main length scale on which velocity correlations decay.

In this work we provide an alternative derivation for the scaling of the viscosity with the coordination deficit δz , the correlation volume, and the characteristic strain scale. Our results are derived for a specific model [the Affine Solvent Model (ASM), where the viscous damping neglects hydrodynamic interactions [7,8] and particles are perfectly hard [11,21]], but they do not require the assumption on the nature of flowing configurations made in Ref. [18]. They also give a natural mechanistic interpretation of several scaling relations near jamming. Our work is based on a detailed

description of the effect of an individual collision between particles on the velocity field and contact forces, which will presumably be of value to understand how perturbations (such as a shear reversal [22]) affect structure and flow. The observation that the mean contact number must not evolve on average implies that a collision (which forms a new contact) must have a finite probability to open exactly one contact, which yields a scaling relation between coordination and viscosity. Our work justifies further why the characteristic finite-size volume varies as $1/\delta z$ [18], as this is precisely the characteristic volume over which the mechanical effect of a collision extends.

In Sec. II we describe the ASM and summarize some of its known properties. Section III shows that imposing the stationarity condition on the average coordination allows us to relate the weakest contact forces in a correlation volume with the characteristic force increment induced by a collision. Sections IV and V study the effect of a collision between particles on the surrounding volume. In Sec. VI we estimate the scale of the weakest contact forces inside the correlation volume obtained in Sec. V, which allows us to establish the scaling relation between the viscosity and the coordination. In Sec. VII we derive the characteristic strain scale at which the particle velocity becomes decorrelated. Finally, in Sec. VIII the marginal stability criterion observed for jammed packing [23,24] is rederived in flows.

II. THE AFFINE SOLVENT MODEL

The ASM is an idealized suspension model which has been shown to have at least qualitatively good agreement with the rheology of dense suspension flows [11]. The model considers N frictionless hard spherical particles in a volume Ω immersed in a viscous fluid of viscosity η_0 , and hydrodynamic interactions are neglected. The viscous fluid acts as a carrier with a velocity profile $\vec{V}^f(\vec{R})$ which depends on the spatial

position \vec{R} . For the sake of simplicity, we shall consider simple shear flow in the x, y plane at constant volume with a strain rate $\dot{\gamma}$, hence $\vec{V}^f(\vec{R}) = \dot{\gamma} y \hat{x}$. The ASM can be easily extended to flows under constant confining pressure instead of constant volume [21]. However, the bulk properties derived in this paper remain unchanged between the two ensembles in the thermodynamic limit.

We consider overdamped dynamics such that the viscous fluid induces a Stokes' drag force proportional to the velocity difference between the particles velocity \vec{V}_k and the fluid velocity $\vec{V}^f(\vec{R}_k)$, where \vec{R}_k is the position of the k th particle. Hence, the drag force is written as

$$\vec{F}_k = -6\pi\eta_0 r_0 [\vec{V}_k - \vec{V}^f(\vec{R}_k)], \quad (1)$$

where r_0 is the mean particle radius. The absence of inertia implies the formation of persistent contacts which form a network as shown in Fig. 1(a). The repulsive contact force between two hard spheres will be taken to be positive. The total number of contacts N_c defines the coordination number $z = 2N_c/N$. In what follows, contacts will be labeled with Greek letters; e.g., the pair of particles i and k in contact will be labeled as β , with the contact force f_β .

The relative radial velocity between particles i and k is given by

$$v_{ik} = (\vec{V}_k - \vec{V}_i) \cdot \vec{n}_{ik}, \quad (2)$$

where the unit vector \vec{n}_{ik} points along the difference $\vec{R}_k - \vec{R}_i$. A positive value of v_{ik} represents pairs of particles moving apart from each other. Hard particles cannot overlap, thus if i is in contact with k , the relative radial velocity v_{ik} must be zero. The resulting set of N_c equations (2) for particles in contact are linear in the N particles' velocities and can be written in a matrix form as

$$S|V\rangle = 0, \quad (3)$$

where S is the $N_c \times ND$ linear operator (D is the spatial dimension) that computes the pairwise velocities v_{ik} between particles in contacts, induced by the particles' velocities \vec{V}_i and \vec{V}_k . The vector $|V\rangle$ of dimension ND represents the velocity field of the entire system, i.e., $\langle i|V\rangle = \vec{V}_i$. Notice that S is a nonsquare matrix which depends only on the unit vectors \vec{n}_{ik} [24]. The velocity profile of the fluid can also be written in compact notation as $|V^f\rangle$, where $\langle k|V^f\rangle = \vec{V}^f(\vec{R}_k)$.

From the expression of the drag force, the requirement that forces are balanced, and the nonoverlap constraints (3) one can compute the instantaneous contact forces [25]:

$$|f\rangle = -6\pi\eta_0 r_0 \dot{\gamma} \mathcal{N}^{-1} |\gamma\rangle, \quad (4)$$

where $\mathcal{N} = SS^t$ and $|\gamma\rangle = S|V^f\rangle/\dot{\gamma}$. $|\gamma\rangle$ is a nonsingular vector of dimension N_c which indicates the imposed deformation mode [see Sec. A of the Appendix for details and for a derivation of Eq. (4)]. In what follows, lowercase vectors correspond to contact-space vectors of dimension N_c , e.g., $f_\beta = \langle \beta|f\rangle$, while uppercase vectors belong to particle space, of dimension ND . The \mathcal{N} matrix depends solely on the geometry of the network formed by the contacts and allows us to determine the rheological properties of the suspension.

The evolution of the system is determined by the velocity field:

$$|V\rangle = \frac{S^t|f\rangle}{6\pi\eta_0 r_0} + |V^f\rangle. \quad (5)$$

The shear stress and the pressure are defined as

$$\sigma \equiv -\frac{\langle \gamma|f\rangle}{\Omega} \quad \text{and} \quad p \equiv \frac{\langle r|f\rangle}{D\Omega} \quad (6)$$

respectively, where $r_\beta \equiv \langle \beta|r\rangle$ is the distance between the particles that form the contact β . Obviously one has

$$\vec{f} \sim r_0^{D-1} p = 6\pi\eta_0 \dot{\gamma} r_0^{D-1} \mathcal{J}^{-1},$$

where $\mathcal{J} = \frac{6\pi\eta_0 \dot{\gamma}}{p}$ is the dimensionless viscous number [3].

Fluctuations of the velocity with respect to the affine flow are given by the nonaffine velocity $|V_{\text{n.a.}}\rangle = |V\rangle - |V^f\rangle$. According to Eqs. (4)–(6), the mean square nonaffine velocity follows $V_{\text{n.a.}}^2 \sim \frac{\dot{\gamma}^2 r_0^D}{\Omega} \langle \gamma|\mathcal{N}^{-1}|\gamma\rangle = \sigma \dot{\gamma} r_0^{D-1}/6\pi\eta_0$. The latter equation simply corresponds to the balance of power injected and power dissipated by the viscous damping [11,12].

In addition, the friction $\mu = \frac{\sigma}{p}$ is known to remain finite at the jamming point; thus as jamming is approached one has

$$p \sim \sigma \sim 6\pi\eta_0 V_{\text{n.a.}}^2 / \dot{\gamma} r_0^{D-1}. \quad (7)$$

For sake of simplicity the typical radius r_0 , the factor $6\pi\eta_0$ and the strain rate $\dot{\gamma}$ will be set to unity in what follows. Therefore, the viscous number controlling the rheology reads $\mathcal{J} = 1/p$ and either \mathcal{J}^{-1} or p can be used interchangeably.

III. STATIONARITY CONDITION

We now discuss the constraint resulting from the fact that in the steady flow state, the average number of contacts (and hence also the coordination z) reaches a stationary value. We observe that around 99% of the contact openings occur due to collisions at all pressures (whose effect is instantaneous since particles are infinitely hard), and only around 1% of the opening take place in between collision. Thus on average, when a collision occurs and a new contact is formed, another contact must open.

To estimate the probability that a contact opens, we must estimate the forces involved in contact formation and destruction. A collision between two particles generates a new contact with a force that we denote f_{coll} . This collision induces a discontinuous change in the surrounding contact forces; the difference $\Delta f_\beta = f_\beta^{\text{after}} - f_\beta^{\text{before}}$ is displayed in Fig. 1(b). Essentially, forming a contact is analogous to imposing a localize dipolar force on a floppy material, a problem we have studied in detail in Refs. [17,26]. In an isostatic system ($\delta z = 0$), a dipole of amplitude f_{coll} would change all forces in the system by $\Delta f_\beta \sim f_{\text{coll}}$. However, in a floppy system ($\delta z > 0$), the amplitude Δf_β is of order of f_{coll} only in the vicinity of the dipole and eventually decays exponentially [17,26]. Therefore, we can define the correlation volume $\Omega_c \equiv (\sum_\beta \Delta f_\beta^2)/f_{\text{coll}}^2$ as the volume inside which the magnitude of Δf_β is of the order of f_{coll} . The change in each force Δf_β can be positive or negative.

At the instance of a collision, the contacts that have a finite probability to open due to the collision are those that reside inside a volume Ω_c around the collision location, and whose

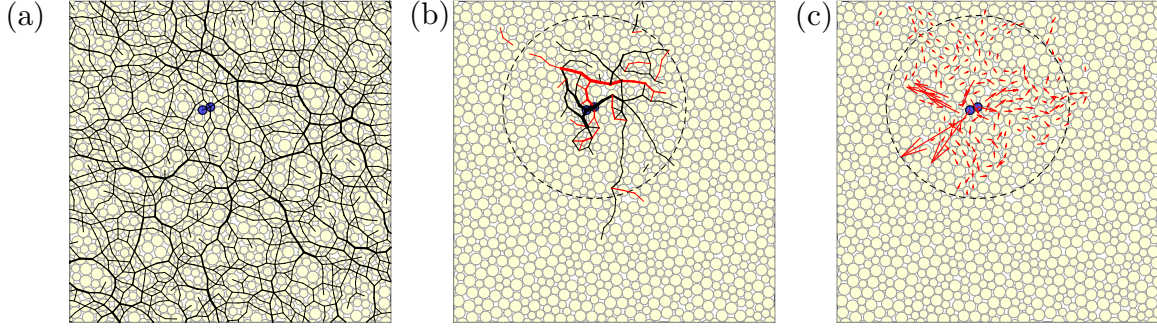


FIG. 1. Snapshot a of suspension flowing under simple shear using the ASM at the instant of a collision between two particles (in blue). (a) Black lines represent the contact network; the width of the lines are proportional to the magnitude of contact forces f immediately after the collision. (b) The width of the lines connecting centers of particles are proportional to the magnitude of the *instantaneous variations* in contact forces induced by the collision. Red (black) lines correspond to negative (positive) variations in the contact forces. The dashed circle is a visualization of the typical volume Ω_c as defined in the text. (c) The vector field represents the *instantaneous variations* in the particles' velocity induced by the collision. The dashed circle is a visualization of the typical volume Ω_v as defined in the text.

force f_{open} before the collision was of order f_{coll} . Thus, f_{open} is expected to scale as f_{coll} , as we confirm in Fig. 2(a) (see Sec. D of the Appendix for details on the numerical method). It is clear from this argument that if $\Omega_c \gg 1$ (which turns out to be true near jamming, see below), then the collisional force f_{coll} must be much smaller than the pressure, and the latter sets the scale of typical contact forces. Otherwise, many contacts inside the volume Ω_c would open upon a typical collision event, which would violate the stationarity of the mean coordination. We thus conclude that the force of the opened contact f_{open} must scale as the *weakest force* in the volume Ω_c [27]. This leads to the scaling relation:

$$f_{\text{min}} \equiv \min_{\in \Omega_c} f \sim f_{\text{coll}}. \quad (8)$$

In what follows we compute f_{coll} , the volume Ω_c and f_{min} to extract a useful scaling relation from Eq. (8).

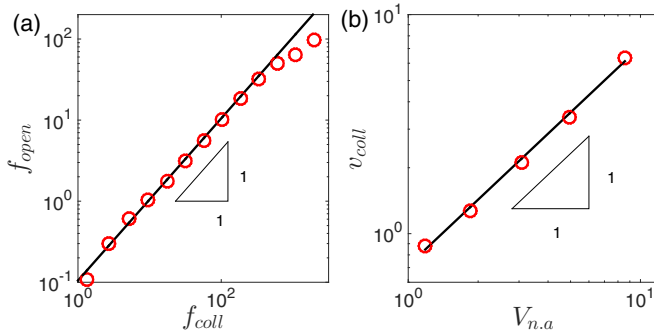


FIG. 2. Data from simulations of the ASM in three dimensions, for systems of $N = 2000$ particles, and pressures of 10, 30, 100, 300, and 1000 (see Sec. D of the Appendix for more details on the numerical method). Solid lines are a guideline to compare data with the theoretical predictions. (a) Forces f_{open} in contacts that open due to a collision, just before the collision takes place, vs the force in the newly created contact f_{coll} . Data are binned according to the measured f_{coll} for all different pressures. (b) Relative radial velocity v_{coll} of pairs of colliding particles just before a collision takes place, vs the mean nonaffine velocity of the particles $V_{n.a}$, taken over all particles in the system. Data are averaged over runs at a certain pressure.

IV. COLLISIONAL FORCE IN THE ASM FRAMEWORK

We expect pairs of particles that are on course to collide not to behave differently than any other pair of particles. If so the relative velocity with which they collide, referred to in what follows as the collisional velocity v_{coll} , must scale as the velocity fluctuations $V_{n.a}$. This assumption is consistent with our numerical observations, as shown in Fig. 2(b). From (7) one gets

$$v_{\text{coll}} \sim \sqrt{p}. \quad (9)$$

When a collision takes place, the relative radial velocity between the colliding particles jumps discontinuously from v_{coll} to 0 (since the particles' velocities must respect the constraint that hard particles cannot overlap), while the force in the contact formed jumps from 0 to some f_{coll} . This discontinuity of the force in the newly formed contact causes a sudden change in the entire force field Δf_β . A collision can open new contacts with a finite probability. However, to estimate the effect of a collision on the force network, we may assume that no contacts open, as this simplification turns out not to modify our estimates.

The operation of \mathcal{S}_a (where the subscripts a and b will refer to the postcollisional and precollisional state, respectively) on the postcollision velocities $|V_a\rangle$ is zero by construction, since the relative radial velocities for particles in contact vanish. However, if \mathcal{S}_a operates on the precollision velocities $|V_b\rangle$, one obtains $\mathcal{S}_a|V_b\rangle = v_{\text{coll}}|\alpha\rangle$, where α is the contact created at the collision. Replacing the constraint (3) by this relation, one obtains the precollision instantaneous response in terms of the contact network after the collision (see Sec. B of the Appendix for details). The precollision contact forces are then given by $|f_b\rangle = -\mathcal{N}_a^{-1}|\gamma\rangle + \mathcal{N}_a^{-1}|\alpha\rangle v_{\text{coll}}$, where $\mathcal{N}_a \equiv \mathcal{S}_a \mathcal{S}_a^t$ and the first term on the right-hand side of the equation corresponds to the postcollision forces $|f_a\rangle$ defined in Eq. (4). Thus, the change in the contact forces is

$$|\Delta f\rangle \equiv |f_a\rangle - |f_b\rangle = -\mathcal{N}_a^{-1}|\alpha\rangle v_{\text{coll}}. \quad (10)$$

From (5) one can also obtain the discontinuous change in the velocity field induced by the collision

$$|\Delta V\rangle \equiv |V_a\rangle - |V_b\rangle = -\mathcal{S}_a^t \mathcal{N}_a^{-1}|\alpha\rangle v_{\text{coll}}. \quad (11)$$

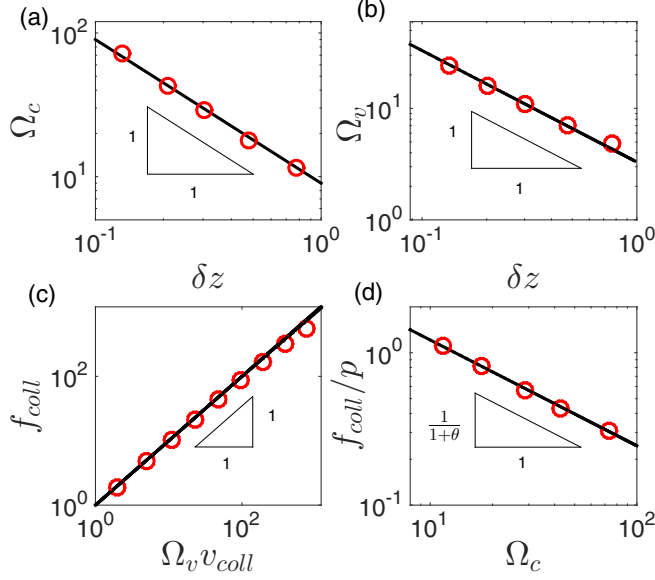


FIG. 3. Data from simulations of the ASM in three dimensions, for systems of $N = 2000$ particles, and pressures of 10, 30, 100, 300, and 1000. Solid lines are a guideline to compare data with the theoretical predictions. (a) The correlation volume Ω_c vs the coordination δz . Data are averaged over runs at a certain pressure. (b) The correlation volume Ω_v vs the coordination δz . Data are averaged over runs at a certain pressure. (c) Mean contact force created at collisions f_{coll} vs the product of the correlation volume Ω_v and the relative radial velocity at the collision v_{coll} . Data are binned according to the measured $\Omega_c v_{\text{coll}}$ for all different pressures. (d) Contact force created upon collisions normalized by the pressure f_{coll}/p vs the correlation volume Ω_c . The exponent $\theta = 0.44$. Data are averaged over runs at a certain pressure.

In Figs. 1(b) and 1(c) we show examples of $|\Delta f|$ and $|\Delta V|$, respectively. By construction, the force in contact α before the collision is zero while the force in α after the collision is precisely f_{coll} ; hence,

$$f_{\text{coll}} = \langle \alpha | \Delta f \rangle = -\Omega_v v_{\text{coll}}, \quad (12)$$

where

$$\Omega_v \equiv \langle \alpha | \mathcal{N}_a^{-1} | \alpha \rangle. \quad (13)$$

In Fig. 3(c) the predicted scaling law (12) is shown to be in very good agreement with our numerics. Notice that $\Omega_v \equiv \frac{\langle \Delta V | \Delta V \rangle}{v_{\text{coll}}^2}$ and can thus be interpreted as the volume where the change on the particles' velocities is of order of the velocity fluctuations V_{na} . In the following section we will show that a single correlation volume exist, hence $\Omega_v \sim \Omega_c \sim 1/\delta z$.

V. CORRELATION VOLUME

The correlation volume Ω_v can be calculated using the spectral decomposition of the \mathcal{N}_a matrix, with ω^2 the eigenvalues and $|r_\omega\rangle$ the respective eigenmode. From the definition of the correlation volume (13) one gets $\Omega_v = \sum_\omega \frac{|\langle \alpha | r_\omega \rangle|^2}{\omega^2}$. The normalization of the eigenmodes implies that $\langle \alpha | r_\omega \rangle \sim$

$1/\sqrt{N_c}$; therefore in the thermodynamic limit

$$\Omega_v \sim \int \frac{D(\omega)}{\omega^2}, \quad (14)$$

where $D(\omega)$ is the eigenfrequencies distribution of the \mathcal{N} matrix. The distribution $D(\omega)$ has been shown to display a plateau above a frequency scale $\omega^* \sim \delta z$ and up to frequencies $\omega \sim O(1)$ [11,17] (modes below ω^* are present but lead to subleading corrections in this argument). Thus one gets from Eq. (14) that $\Omega_v \sim \frac{1}{\delta z}$, as shown in Fig. 3(b). Together with (12) and (9), one gets from this result

$$f_{\text{coll}} \sim \frac{\sqrt{p}}{\delta z}. \quad (15)$$

The correlation volume

$$\Omega_c \equiv \frac{\langle \Delta f | \Delta f \rangle}{f_{\text{coll}}^2} \sim \delta z^2 \langle \alpha | \mathcal{N}_a^{-2} | \alpha \rangle \quad (16)$$

can be calculated in a similar way:

$$\Omega_c \sim \delta z^2 \sum_\omega \frac{|\langle \alpha | r_\omega \rangle|^2}{\omega^4} \sim \delta z^2 \int_{\omega^*}^1 \frac{D(\omega)}{\omega^4} \sim 1/\delta z.$$

Thus both correlation volumes scale identically:

$$\Omega_c \sim \Omega_v \sim \frac{1}{\delta z} \quad (17)$$

as shown in Fig. 3(a).

VI. WEAKEST FORCE IN THE VOLUME Ω_c

It was recently shown that mechanical stability requires the distribution of contact forces in packings of frictionless spheres to vanish at small forces [23], as observed in Ref. [25]. There is one subtlety, however: contacts at low forces can be decomposed in two types: some are mechanically isolated, whereas others are coupled mechanically to the rest of the system [24,28]. Only the latter are relevant for the present argument. For those one finds

$$P(f/p) \sim \left(\frac{f}{p}\right)^\theta$$

with $\theta \approx 0.44$ [24]. This result can be derived in infinite dimension using the replica trick [29], yielding a similar result $\theta \approx 0.42$ that appears to be correct in any dimensions.

Considering that the force distribution in flow must converge to that of jammed packings as the jamming point is approached, the minimum force f_{min} can be easily estimated. Indeed, the number of contact forces inside the correlation volume is proportional to Ω_c . The weakest force f_{min} can be estimated by the relation $\frac{1}{\Omega_c} \sim \int_0^{f_{\text{min}}/p} P(b) db$, which leads to $\frac{f_{\text{min}}}{p} \sim \Omega_c^{-\frac{1}{1+\theta}}$. Using the stationarity condition (8) one gets

$$\frac{f_{\text{coll}}}{p} \sim \Omega_c^{-\frac{1}{1+\theta}}, \quad (18)$$

which is in good agreement with the data shown in Fig. 3(d).

Finally, from the relations (18), (15), and (17), one obtains scaling relations relating structure to rheological and dynamical properties:

$$\delta z \sim p^{-\frac{1+\theta}{(4+2\theta)}} \sim p^{-0.30}, \quad (19)$$

$$\Omega_c \sim p^{\frac{1+\theta}{4+2\theta}} \sim p^{0.30}, \quad (20)$$

$$f_{\text{coll}} \sim p^{\frac{3+2\theta}{4+2\theta}} \sim p^{0.80}. \quad (21)$$

Equation (19) was tested numerically in Ref. [18]. Equation (19) combined with Fig. 3(a) verifies Eq. (20), and the latter equation combined with Fig. 3(d) verifies Eq. (21).

VII. STRAIN SCALE BETWEEN COLLISION IN Ω_c

The strain $\Delta\gamma_c$ between two consecutive collision in a volume Ω_c can be obtained from the stationarity of the shear stress in the steady flow state. The increase in the shear stress $\Delta\sigma$ induced by a collision that forms some contact α can be computed from Eq. (6) and Eq. (10):

$$\Delta\sigma = -\frac{\langle\gamma|\Delta f\rangle}{\Omega} = v_{\text{coll}} \frac{\langle\gamma|\mathcal{N}_a^{-1}|\alpha\rangle}{\Omega}. \quad (22)$$

Before the formation of the contact α , no forces are exerted between those particles, hence from Eq. (10) one gets $\langle\alpha|\mathcal{N}_a^{-1}|\alpha\rangle v_{\text{coll}} = \langle\alpha|\mathcal{N}_a^{-1}|\gamma\rangle$. The jump in the shear stress then scales as $\Delta\sigma \sim \frac{v_{\text{coll}}^2 \Omega_c v}{\Omega} \sim \frac{p}{\delta z \Omega}$. The stress relaxes between collisions, following $\frac{d\sigma}{d\gamma} \sim -\sigma^2 \sim -p^2$, as shown in Ref. [17]. Stationarity then implies that the strain scale between two consecutive collision in the entire system must scale as $\Delta\sigma/\frac{d\sigma}{d\gamma} \sim \frac{1}{\delta z p \Omega}$. Therefore, the strain scale $\Delta\gamma_c$ between two consecutive collision in a volume Ω_c is given by

$$\Delta\gamma_c \sim \frac{1}{\delta z p \Omega_c} \sim \frac{1}{p}. \quad (23)$$

A collision induces a change in the velocity field, inside the correlation volume Ω_c , on the order of the nonaffine velocity. Thus, it is expected that the velocity correlations (with respect to strain) start to decorrelate precisely at a strain scale on the order of $\Delta\gamma_c$ (see Sec. C of the Appendix), as observed in Refs. [17,30].

VIII. RECOVERING MARGINAL STABILITY IN FLOW

Stationarity also imposes a constraint between the particles' displacements and the gaps between particles in suspension flows. Close to the jamming point the relative velocity between particles scales as the nonaffine velocities. Then the relative displacements that take place in a strain scale $\Delta\gamma_c$ between consecutive collisions inside the correlation volume Ω_c scale as $\Delta\gamma_c V_{na}$. Such displacements must be of the same order as the minimal gap h_{min} inside Ω_c :

$$h_{\text{min}} \equiv \min_{\in \Omega_c} h \sim \Delta\gamma_c V_{na}. \quad (24)$$

The gap distribution at scales smaller than Ω_c is expected to be the same as for jammed packing. The distribution of jammed packing at small gaps is known to rise as a power law $P(h) \sim h^\nu$ with $\nu \approx 0.38$ [24,25,31]. Then the minimal gap inside a

volume Ω_c is given by the relation $\frac{1}{\Omega_c} \sim \int_0^{h_{\text{min}}} h^{-\nu} dh$, from which we obtain $h_{\text{min}} \sim \Omega_c^{-\frac{1}{1-\nu}}$. Using this relation together with Eqs. (7), (17), (24), and (23), one gets

$$p \sim \delta z^{-\frac{2}{1-\nu}}, \quad (25)$$

which is a second, independently derived expression that connects the suspension's macroscopic pressure with its microstructure. Comparing Eqs. (25) and (19), one finds that the exponents θ and ν must be related by $\frac{1}{1-\nu} = \frac{2+\theta}{1+\theta}$. This relation between exponents was previously established for jammed packings and was shown to be a consequence of their intrinsic marginal stability [23,24]. The extension of this relation below the jamming critical point can be interpreted as follows: suspension flows remain "marginally stable" far from the jamming point at scales smaller than Ω_c .

IX. DISCUSSION AND CONCLUSION

We have formulated a microscopic scaling theory for dense non-Brownian suspension rheology in the framework of the ASM. We build upon the stationarity of the collisional processes in steady flow states to establish several scaling relations between the pressure, coordination, strain scales, and correlation volumes. The constitutive relations, known as the friction and dilatancy laws, can be derived via finite size scaling arguments and the assumption of perturbation around a jammed solid [18]. Obtaining them in the present approach that focuses on collisions would be very interesting.

In previous works [17,26] we showed that local perturbations, as well as velocity correlations, decay exponentially at distance $r > \xi \sim \frac{1}{\sqrt{\delta z}}$. However, the effective volume affected by a local perturbation we computed here is given by $\Omega_c \sim 1/\delta z$, which is much smaller (except in two dimensions) than the naive correlation volume given by ξ^d . There is no contradiction: it simply signals that the leading term of the response to a contact forming decays with distance r as $\delta R_\alpha^2(r) \sim f(r/\xi)/r^{d-2}$, where $f(x)$ is a rapidly decaying function of its argument.

Finally, a central question is how universal the present results are. First, we expect our results on the spatial effects of collisions to hold true when *inertia* is present. Indeed, in the unified description of viscous flows and inertial flows of frictionless particles we proposed in Ref. [18], the properties of the contact network (which control collisions) are essentially the same in these two cases. Second, and most importantly, we also expect that in the suspension case, both our results on collisions as well as those of Ref. [18] hold true when particles are *frictional*. This is not obvious at all, because in the inertial case friction affects the scaling exponents near jamming [32,33]. However, in the presence of inertia, the change of scaling behavior stems from a change in the dominant dissipation mechanism, which becomes dominated by friction instead of collisions close to jamming [34]. However, in suspensions friction does not appear to dominate dissipation in the range of viscous numbers probed by numerics [13] and experiments [20]. We thus expect our results to hold in real materials in that range, where they could be tested via imaging with sufficient temporal and spatial resolution.

ACKNOWLEDGMENTS

We thank Eric DeGiuli, L. Yan, J. Lin, and M. Battalia for discussions. G.D. acknowledges support from FONDECYT Grant No. 1150463. E.L. acknowledges funding from the Amsterdam Academic Alliance fellowship. M.W. thanks the Swiss National Science Foundation for support under Grant No. 200021-165509 and the Simons Collaborative Grant.

APPENDIX

1. Contact forces in the affine solvent model

The ASM is an idealized suspension model which considers N frictionless hard spherical particles in a volume Ω , immersed in a viscous fluid, and hydrodynamic interactions are neglected. The dynamics is overdamped, and the viscous drag force is proportional to the velocity difference between the particles and the fluid velocity. The drag force (1) can be written in compact form using bracket notation:

$$|F\rangle = -6\pi\eta_0 r_0 (|V\rangle - |V^f\rangle). \quad (\text{A1})$$

In addition to the drag force, particles in contact interact via repulsive contact forces. The force acting over particle k due to particle i is given by $f_{ik}\vec{n}_{ik}$ where f_{ik} represents the amplitude of the contact force (taken to be positive), and \vec{n}_{ik} points along the difference vector $\vec{R}_k - \vec{R}_i$. Since we consider overdamped dynamics, the drag force on each particle is balanced at all times by the contact forces exerted by other particles, hence

$$\vec{F}_k + \sum_{i \neq k} f_{ik}\vec{n}_{ik} = 0. \quad (\text{A2})$$

Interaction forces in hard sphere systems are different from zero only for particles which are in contact. Thus the sum in (A2) runs only over the particles in contact, which can be written in compact notation using the transpose of the \mathcal{S} operator [21]:

$$|F\rangle + \mathcal{S}^t |f\rangle = 0. \quad (\text{A3})$$

Operating with the \mathcal{S} matrix on both side of the above equation, and using expression (A1) one finds

$$-6\pi\eta_0 r_0 \mathcal{S}|V\rangle + 6\pi\eta_0 r_0 \mathcal{S}|V^f\rangle + \mathcal{S}\mathcal{S}^t |f\rangle = 0.$$

The constraints imposed by the hard spheres as described by Eq. (3) imply that the first term in the above equation vanishes. Defining the matrix $\mathcal{N} = \mathcal{S}\mathcal{S}^t$ and denoting the relative radial velocity induced by the fluid as $|v^f\rangle = \mathcal{S}|V^f\rangle$, the fundamental equation of the ASM for the contact forces is obtained as

$$|f\rangle = -6\pi\eta_0 r_0 \mathcal{N}^{-1} |v^f\rangle. \quad (\text{A4})$$

For a simple shear flow $|v^f\rangle = \dot{\gamma}|\gamma\rangle$ where the components of the vector $|\gamma\rangle$ are given by $||\vec{R}_k - \vec{R}_i||(\vec{n}_{ik} \cdot \vec{e}_x)(\vec{n}_{ik} \cdot \vec{e}_y)$. Together with the contact forces $|f\rangle$, we determine the key

rheological observables of the suspension, and in particular:

$$\text{drag force } |F\rangle = 6\pi\eta_0 r_0 \mathcal{S}^t \mathcal{N}^{-1} |v^f\rangle, \quad (\text{A5})$$

$$\text{velocity } |V\rangle = -\mathcal{S}^t \mathcal{N}^{-1} |v^f\rangle + |V^f\rangle, \quad (\text{A6})$$

$$\text{pressure } p \equiv \frac{\langle r|f\rangle}{D\Omega} = -6\pi\eta_0 r_0 \frac{\langle r|\mathcal{N}^{-1}|v^f\rangle}{D\Omega}, \quad (\text{A7})$$

$$\text{shear stress } \sigma \equiv -\frac{\langle \gamma|f\rangle}{\Omega} = 6\pi\eta_0 r_0 \frac{\langle \gamma|\mathcal{N}^{-1}|v^f\rangle}{\Omega}. \quad (\text{A8})$$

A simple shear velocity profile preserves the packing fraction ϕ , while the pressure fluctuates around some mean value in steady-state flows. Such fluctuations can become very large close to the jamming point due to finite size effects. In some situations it is therefore advantageous to consider a constant pressure system in which the packing fraction fluctuates around some mean. This can be done in the ASM framework by allowing the system to dilate and contract in addition to the simple shear velocity profile [21]. The relative radial velocity of the fluid is then given by $|v^f\rangle = \dot{\gamma}(|\gamma\rangle + \kappa|r\rangle)$ where κ is the dilatancy per unit shear, and the latter is determined by imposing a constant pressure in Eq. (A7). The result is

$$\kappa = \frac{pD\Omega/\dot{\gamma}6\pi\eta_0 r_0 - \langle r|\mathcal{N}^{-1}|\gamma\rangle}{\langle r|\mathcal{N}^{-1}|r\rangle}.$$

The constitutive equations as well as the bulk properties should not depend on the ensemble considered, whether the constant pressure or constant packing fraction ensemble. Nevertheless, some properties might depend on the nature of the boundary conditions such as the fluctuations or relaxation of global quantities. In this work, unless otherwise stated, the results are valid in both cases.

2. Force change induced by particle collision

As stated in the main text, operating with the postcollisional \mathcal{S}_a matrix on the precollisional velocities $|V_b\rangle$, one obtains

$$\mathcal{S}_a |V_b\rangle = v_{\text{coll}} |\alpha\rangle, \quad (\text{A9})$$

where α is the contact created in the collision. Since the force between a pair of particles that are not in contact is zero, the force balance condition (A3) can be rewritten as

$$|F_b\rangle + \mathcal{S}_a^t |f_b\rangle = 0,$$

where $\langle \alpha|f_b\rangle = 0$. Operating on both sides of the above equation by \mathcal{S}_a and using the drag force definition Eq. (1), one finds

$$-\mathcal{S}_a |V_b\rangle + \mathcal{S}_a |V^f\rangle + \mathcal{S}_a \mathcal{S}_a^t |f_b\rangle = 0,$$

which is similar to the expression found in the last section. Notice that $6\pi\eta_0$ and r_0 were set to unity. Replacing Eq. (A9) in the above equation leads to the expression used in the main text:

$$|f_b\rangle = -\mathcal{N}_a^{-1} |v^f\rangle + \mathcal{N}_a^{-1} |\alpha\rangle v_{\text{coll}}, \quad (\text{A10})$$

where $\mathcal{N}_a = \mathcal{S}_a \mathcal{S}_a^t$ and $|v^f\rangle = \mathcal{S}_a |V^f\rangle$.

3. Decorrelation strain scale

We define the nonaffine velocity correlation function as

$$C(\gamma_0, \gamma) = \frac{\langle V_{n.a}^0 | V_{n.a} \rangle}{\sqrt{\langle V_{n.a}^0 | V_{n.a}^0 \rangle \langle V_{n.a} | V_{n.a} \rangle}},$$

where $V_{n.a}^0$ and $V_{n.a}$ denote the nonaffine velocities at the strains γ_0 and γ , respectively. We aim at determining the difference $\Delta C = C(\gamma_0, \gamma + \delta\gamma) - C(\gamma_0, \gamma)$ which can be written as

$$\Delta C = C(\gamma_0, \gamma) \left[\frac{\left(1 + \frac{\langle V_{n.a}^0 | \Delta V \rangle}{\langle V_{n.a}^0 | V_{n.a} \rangle}\right)}{\sqrt{\left(1 + \frac{2\langle V_{n.a} | \Delta V \rangle}{\langle V_{n.a} | V_{n.a} \rangle} + \frac{\langle \Delta V | \Delta V \rangle}{\langle V_{n.a} | V_{n.a} \rangle}\right)}} - 1 \right],$$

where the velocity field at $\gamma + \delta\gamma$ is given by $|V_{n.a}\rangle + |\Delta V\rangle$. In Sec. VII we showed that the strain scale between collisions is given by $\delta\gamma = \frac{1}{\delta z p \Omega}$. We thus estimate the change in the velocity field as the change induced by a collision (11) plus the change of the velocities between collisions. Between collisions the velocities vary smoothly, hence the change in the velocity field between collisions is approximately given by $|\partial_\gamma V(\gamma)\rangle \delta\gamma$. Thus to the lowest order in $\delta\gamma$ the correlation function can be approximated as

$$\Delta C \approx C(\gamma_0, \gamma) \left(\frac{\langle V_{n.a}^0 | \Delta V \rangle}{\langle V_{n.a}^0 | V_{n.a} \rangle} - \frac{v_{\text{coll}}^2}{2} \frac{\langle \alpha | \mathcal{N}_a^{-1} | \alpha \rangle}{\langle V_{n.a} | V_{n.a} \rangle} \right). \quad (\text{A11})$$

In the last expression we used that $\langle V_{n.a} | \Delta V \rangle = 0$ in a collision, as can be shown using Eq. (11), and we assume that

$\langle V_{n.a} | \partial_\gamma V \rangle \sim N^\nu$ with $\nu < 1$. In general the scaling properties of $\frac{\langle V_{n.a}^0 | \Delta V \rangle}{\langle V_{n.a}^0 | V_{n.a} \rangle}$ are unknown. However, while the correlation function $C(\gamma_0, \gamma) \sim 1$ the velocity $V_{n.a}^0$ can be approximated by $V_{n.a}$, and the first term on the left-hand side of Eq. (A11) can be neglected. We finally find that the initial evolution of the correlation function is given by

$$\Delta C \approx -\frac{v_{\text{coll}}^2}{2} \frac{\langle \alpha | \mathcal{N}_a^{-1} | \alpha \rangle}{\langle V_{n.a} | V_{n.a} \rangle} C(\gamma_0, \gamma) \sim -\frac{1}{\delta z N} C(\gamma_0, \gamma).$$

Since $\delta\gamma = \frac{1}{\delta z p \Omega} \sim \frac{1}{\delta z p N}$ one can rewrite the last expression as

$$\Delta C \sim -p C(\gamma_0, \gamma) \delta\gamma.$$

In the limit of large N the above expression represents a differential equation, the solution to which displays an exponential decay with strain over a decorrelation strain scale of $\frac{1}{p}$.

4. Numerical methods

Data for the ASM were generated using the algorithm described in Ref. [21]. We have simulated a binary mixture of large and small spheres in three dimensions with $N = 2000$, setting the ratio of radii of large and small particles to 1.4. Systems were deformed under simple shear with Lees-Edwards periodic boundary conditions. We simulated systems at various pressures ranging from $p = 10$ to $p = 1000$. Rattlers have been removed from the analysis; see Ref. [21] for details about the procedure of rattlers removal.

-
- [1] A. Einstein, *Ann. Phys.* **324**, 289 (1906).
[2] E. Brown and H. M. Jaeger, *Phys. Rev. Lett.* **103**, 086001 (2009).
[3] F. Boyer, E. Guazzelli, and O. Pouliquen, *Phys. Rev. Lett.* **107**, 188301 (2011).
[4] O. Pouliquen, *Phys. Rev. Lett.* **93**, 248001 (2004).
[5] R. Lespiat, S. Cohen-Addad, and R. Höhler, *Phys. Rev. Lett.* **106**, 148302 (2011).
[6] K. N. Nordstrom, E. Verneuil, P. E. Arratia, A. Basu, Z. Zhang, A. G. Yodh, J. P. Gollub, and D. J. Durian, *Phys. Rev. Lett.* **105**, 175701 (2010).
[7] D. J. Durian, *Phys. Rev. Lett.* **75**, 4780 (1995).
[8] P. Olsson and S. Teitel, *Phys. Rev. Lett.* **99**, 178001 (2007).
[9] P. Olsson and S. Teitel, *Phys. Rev. E* **83**, 030302 (2011).
[10] T. Hatano, *Phys. Rev. E* **79**, 050301(R) (2009).
[11] E. Lerner, G. Düring, and M. Wyart, *Proc. Natl. Acad. Sci. USA* **109**, 4798 (2012).
[12] B. Andreotti, J.-L. Barrat, and C. Heussinger, *Phys. Rev. Lett.* **109**, 105901 (2012).
[13] M. Trulsson, B. Andreotti, and P. Claudin, *Phys. Rev. Lett.* **109**, 118305 (2012).
[14] D. Vågberg, P. Olsson, and S. Teitel, *Phys. Rev. Lett.* **113**, 148002 (2014).
[15] A. Ikeda, L. Berthier, and P. Sollich, *Phys. Rev. Lett.* **109**, 018301 (2012).
[16] M. Wang and J. F. Brady, *Phys. Rev. Lett.* **115**, 158301 (2015).
[17] G. Düring, E. Lerner, and M. Wyart, *Phys. Rev. E* **89**, 022305 (2014).
[18] E. DeGiuli, G. Düring, E. Lerner, and M. Wyart, *Phys. Rev. E* **91**, 062206 (2015).
[19] D. Vågberg, P. Olsson, and S. Teitel, *Phys. Rev. E* **93**, 052902 (2016).
[20] S. Dagois-Bohy, S. Hormozi, É. Guazzelli, and O. Pouliquen, *J. Fluid Mech.* **776**, R2 (2015).
[21] E. Lerner, G. Düring, and M. Wyart, *Comput. Phys. Commun.* **184**, 628 (2013).
[22] F. Blanc, F. Peters, and E. Lemaire, *J. Rheol.* **55**, 835 (2011).
[23] M. Wyart, *Phys. Rev. Lett.* **109**, 125502 (2012).
[24] E. Lerner, G. Düring, and M. Wyart, *Soft Matter* **9**, 8252 (2013).
[25] E. Lerner, G. Düring, and M. Wyart, *EPL (Europhys. Lett.)* **99**, 58003 (2012).
[26] G. Düring, E. Lerner, and M. Wyart, *Soft Matter* **9**, 146 (2013).
[27] This argument is somewhat more subtle, because some contacts that carry a weak force are mechanically isolated and are thus insensitive to collisions. Only the contacts mechanically coupled to the rest of the system have to be considered in this argument; see Ref. [24].

- [28] P. Charbonneau, E. I. Corwin, G. Parisi, and F. Zamponi, *Phys. Rev. Lett.* **114**, 125504 (2015).
- [29] P. Charbonneau, J. Kurchan, G. Parisi, P. Urbani, and F. Zamponi, *Nat. Commun.* **5**, 3725 (2014).
- [30] P. Olsson, *Phys. Rev. E* **81**, 040301 (2010).
- [31] P. Charbonneau, E. I. Corwin, G. Parisi, and F. Zamponi, *Phys. Rev. Lett.* **109**, 205501 (2012).
- [32] P.-E. Peyneau and J.-N. Roux, *Phys. Rev. E* **78**, 011307 (2008).
- [33] F. Radjai and S. Roux, Contact dynamics study of 2d granular media: Critical states and relevant internal variables, *The Physics of Granular Media* (Wiley, New York, 2005), pp. 165–187.
- [34] E. DeGiuli, J. N. McElwaine, and M. Wyart, *Phys. Rev. E* **94**, 012904 (2016).